

Electronic Supplementary Information for

Interactions Between Th(IV) and Graphene Oxide: Experimental and Density Functional Theoretical Investigations

Zhi-Qiang Bai^{a,b}, Zi-Jie Li^a, Cong-Zhi Wang^a, Li-Yong Yuan^a, Zhi-Rong Liu^b, Jing Zhang^c, Li-Rong Zheng^c, Yu-Liang Zhao^a, Zhi-Fang Chai*^{a,d} and Wei-Qun Shi*^a

^a **Group of nuclear energy nano-chemistry, Key Laboratory of Nuclear Radiation and Nuclear Energy Technology and Key Laboratory for Biomedical Effects of Nanomaterials and Nanosafety, Institute of High Energy Physics, Chinese Academy of Sciences, Beijing 100049, China.**

^b **School of Nuclear Engineering and Geophysics, East China Institute of Technology, Nanchang 330013, China**

^c **Beijing Synchrotron Radiation Facility, Institute of High Energy Physics, Chinese Academy of Sciences , Beijing 100049, China**

^d **School of Radiological& Interdisciplinary Sciences, Soochow University, Suzhou 215123, China**

Corresponding Author

E-mail: shiwq@ihep.ac.cn; zfchai@suda.edu.cn

S-1. Details for synthesis of GO

Graphite oxide (GO) was prepared from natural graphite powder (Alfa Aesar, > 99.9995%) by the Hummers method using NaNO₃, H₂SO₄, and KMnO₄.¹ The oxidation product was purified by rinsing with a 10% HCl solution, repeatedly washing with copious amounts of ultrapure water, and filtering through 0.22 µm nylon filter paper. The filter cake was dried under vacuum (80 °C, 3 h) and the GO solid was obtained. Or re-dispersing the filter cake in ultrapure water with mild sonication (150 W, 4 h), then the exfoliated GO was obtained. The suspension was centrifuged at 4000 rpm for 20 min, and the supernatant was collected as a stock solution, which was used in the following sorption experiments.

S-2. Characterization methods

The AFM images of GO were obtained in air by using a Veeco Nanoscope 5 system (Veeco Metrology) in a tapping mode. All the AFM samples were prepared by dripping a GO suspension (~0.02 g/L) on a silicon wafer, followed by drying in air. The morphology of GO was observed with SEM (S-4800, HITACHI) at an accelerating voltage of 1.0 kV. FT-IR spectroscopic measurements were amounted by using a PerkinElmer Spectrum GX FTIR system in KBr pellet. The XPS spectra were recorded on a scanning X-ray microprobe (PHI Quantera, ULVAC-PHI, Inc) with an Al K_α source ($E=1486.7\text{eV}$). Raman spectra were recorded from 3500 to 800 cm⁻¹ on a Renishaw RM 2000 Microscopic Confocal Raman spectrometer with a 514 nm argon ion laser.

S-3. The kinetic models.

The linear form of the pseudo-first-order and the pseudo-second-order are expressed as followed respectively.

$$\text{The pseudo-first-order equation: } \log(q_e - q_t) = \log q_e - \frac{k_1 t}{2.303} \quad (\text{S1})$$

$$\text{The pseudo-second-order equation: } \frac{t}{q_t} = \frac{1}{k_2 q_e^2} + \frac{t}{q_t} \quad (\text{S2})$$

where q_e (mg/g) and q_t (mg/g) are the quantities of the sorbed Th(IV) at equilibrium and at time t respectively, k₁ (1/min) and k₂ (g/(mg·min)) are the pseudo-first-order

and pseudo-second-order sorption rate constants.

S-4. The Langmuir and Freundlich isotherm models.

The Langmuir model assumes that the sorption of metal ions occurs on a homogenous surface by monolayer sorption and there no interaction between adsorbed ions, with homogeneous binding sites and equivalent sorption energies. The linear equation of the Langmuir isotherm model is expressed as followed:

$$\frac{C_e}{q_e} = \frac{1}{q_m k_L} + \frac{C_e}{q_m} \quad (\text{S3})$$

where q_m is the maximum sorption capacity corresponding to complete monolayer coverage (mg/g) and k_L is a constant indirectly related to sorption capacity and energy of sorption (L/mg), which characterizes the affinity of the adsorbate with the adsorbent. The linearized plot was obtained when we plotted C_e/q_e against C_e and q_m and k_L could be calculated from the slope and intercept.

The Freundlich equation is an empirical equation with the assumption of sorption on a heterogeneous surface. The linear equation can be expressed by:

$$\ln q_e = \ln k_F + \frac{1}{n} \ln C_e \quad (\text{S4})$$

where k_F and n are the Freundlich constants related to the sorption capacity and the sorption intensity, respectively. The linear plot was obtained by plotting $\ln q_e$ against $\ln C_e$, and the values of k_F and n were calculated from the slope and intercept of the straight line.

S-5. Calculation of Thermodynamic Data.

The standard Gibbs free energy (ΔG^0), standard enthalpy (ΔH^0) and entropy (ΔS^0) can be calculated from the equations followed:

$$\ln K_d = \frac{\Delta S^0}{R} - \frac{\Delta H^0}{RT} \quad (\text{S5})$$

$$\Delta G^0 = \Delta H^0 - T\Delta S^0 \quad (\text{S6})$$

where K_d is the distribution coefficient (ml/g) of Th(IV) in sorbent and in solution, T represents the absolute temperature (K), and R denotes the ideal gas constant (8.314 J/(mol·K)).

S-6. Samples preparation and analysis of EXAFS data

The reference sample of precipitate of Th(IV) hydrous oxide or hydroxide was prepared in air by slow titration of a thorium nitrate solution with NaOH. The samples of Th(IV)-loaded GO for EXAFS measurement were prepared in the same batch experiments. After sorption processes, samples were centrifuged at 10000 rpm for 1 h to concentrate the solid phases. The sediments were mounted in the holes of Teflon sample holders, sealed with Kapton tape, and subjected to EXAFS measurements. A silicon (111) double-crystal monochromator was used to tune the incident X-ray beam to the desired energies. EXAFS data analysis is based on standard least-squares fitting techniques using the Athena software. The region to about 700 eV above the Th L3-edge ($k \sim 13.5 \text{ \AA}^{-1}$) is investigated. Rbkg 1.2 was used to optimize the atomic background function (μ_0) using the autobk utility. To extract metric parameters (neighboring atomic distances \AA , EXAFS Debye-Waller factors (σ^2), coordination numbers (N)) from the EXAFS, the theoretical phase shift and amplitude functions for single and double scattering paths are calculated by the program FEFF6 and optimized as implemented in the FEFFIT code using the model structure of thorium oxalate. Prior to analysis, the k^3 -weighted EXAFS spectra are Fourier transformed over a k-space range of $\sim 2.9\text{-}9.7 \text{ \AA}^{-1}$, using symmetric square windows with $\Delta k = 0.1 \text{ \AA}^{-1}$ “Hanning sills”. All the fitting operations are performed in R-space over the individual radial distance ranges of $\sim 1.47\text{-}2.8 \text{ \AA}$.

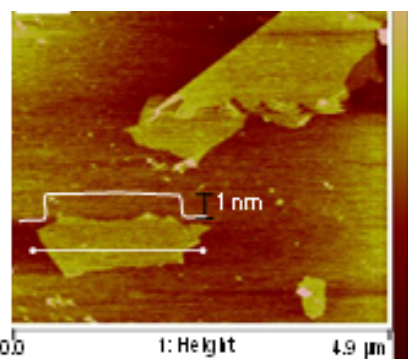


Figure S1. AFM image of GO

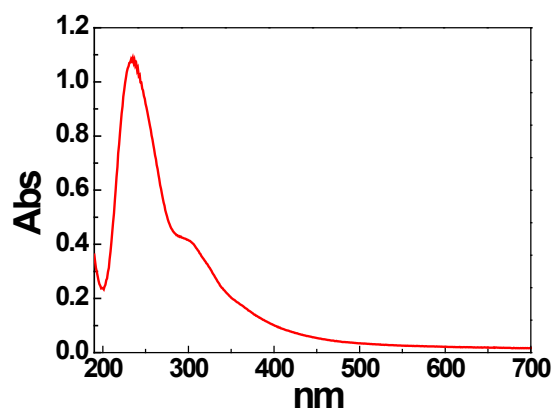


Figure S2. UV-Vis spectra of GO. Peaks at about 230 nm and a shoulder at 300 nm, which correspond to the $\pi-\pi^*$ transition of aromatic C=C bonds and the $n-\pi^*$ transition of C=O bonds

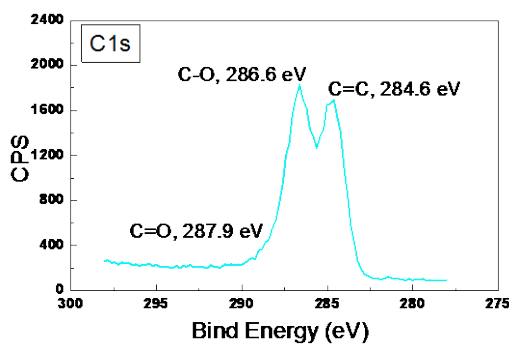


Figure S3. GO C1s XPS analysis. 284.8 (48.4%), 286.6 (47.6%), and 287.9 eV (4.0%) were assigned to the graphitic C=C bonds, C-O and C=O functional groups, respectively

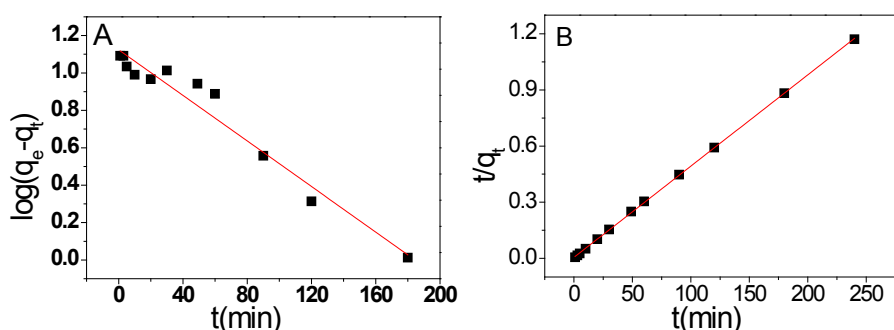


Figure S4. (A) The pseudo-first-order kinetic model and (B) pseudo-second-order kinetic model linearized plots for Th (IV) sorption on GO.

Table S1. The kinetic constants of the Th(IV) sorption onto GO.

pseudo-first-order kinetic model			pseudo-second-order kinetic model		
q_e (mg/g)	K_1 (/min)	R^2	q_e (mg/g)	K_2 (g/mg/min)	R^2
13.29	0.014	0.954	204.92	0.0048	0.999

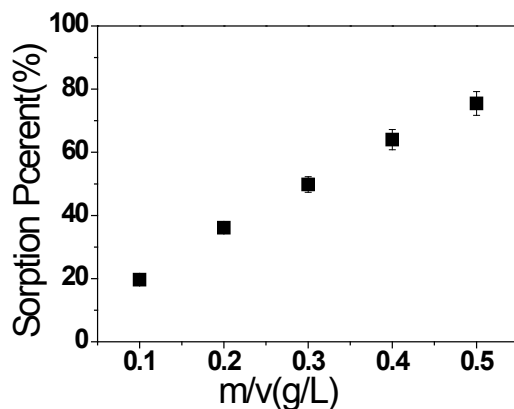


Figure S5. The effect of solid-to-liquid ratio on the Th(IV) sorption on GO. $C_0(\text{Th})=120$ mg/L and pH=2.6±0.05.

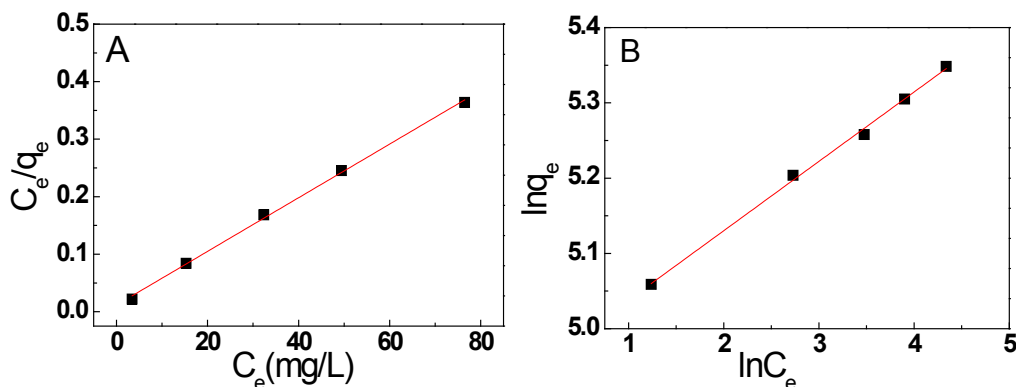


Figure S6. (A) Langmuir isotherm and (B) Freundlich isotherm models linearized plots for Th(IV) sorption on GO.

Table S2. The Langmuir isotherm and Freundlich isotherm models constants of the Th(IV) sorption onto GO.

Langmuir		Freundlich		
q_m (mg/g)	k_L (L/mg)	R^2	k_F (mg/g)	n
214.6	0.402	0.998	140.6	10.857

Table S3. Maximum sorption capacity of various sorbents for Th(IV) ions

Sorbents	Q_{\max} (mg/g)	Conditions	References
composite matrix	110.5	pH 5.5, 303K	2
Al-MCM-41	~70	pH 3.4 ± 0.1, 293K	3
calcined diatomite	121.22	pH 4.0, 298K	4
activated carbon	21.28	pH 4.0, 303K	5
Amine modified silica gel	96	pH 3.5, 298K	6
tannin-modified poly(glycidylmethacrylate)-grafted zirconium oxide-densified cellulose	96.7	pH 5.5 ,303K	7
GO	214.6	pH 2.60±0.05, 293K	This work

Table S4. Average bond lengths (\AA) of optimized binding geometries for the coordination of Th(IV) with GO by the B3LYP Method.

motifs	A	B	C	D	E	F	G
Th-O(COOH ⁻ /OH ⁻)	2.303	2.506	2.469	2.356	2.429	2.567	2.524
Th-O(NO ₃ ⁻)	2.456	2.436	2.442	2.497	2.487	2.475	2.481

Table S5. Mayer Bond Orders (MBO) of Th-O bonds and Natural Charges on the Th and O atoms for the complexes obtained by the B3LYP method.

motifs	Th-O _C	Th-O _N	Q(Th)	Q(O _C)	Q(O _N)
A	0.458	0.405	1.958	-0.772	-0.521
B	0.257	0.434	1.007	-0.381	-0.262
C	0.325	0.424	1.992	-0.802	-0.522
D	0.402	0.375	1.776	-0.729	-0.491
E	0.311	0.381	1.809	-0.673	-0.495
F	0.210	0.395	1.817	-0.720	-0.496
G	0.276	0.388	1.796	-0.750	-0.492

Reference

- 1 L. J. Cote, F. Kim and J. Huang, *J. Am. Chem. Soc.*, 2008, **131**, 1043-1049.
- 2 T. S. Anirudhan, S. Rijith and V. R. N. Ratheesh, *Desalin. Water Treat.*, 2012, **38**, 79-89.
- 3 L. Zuo, S. Yu, H. Zhou, X. Tian and J. Jiang, *J. Radioanal. Nucl. Chem.*, 2011, **288**, 379-387.
- 4 S. Yusan, C. Gok, S. Erenturk and S. Aytas, *Appl. Clay. Sci.*, 2012, **67-68**, 106-116.
- 5 C. Kuumltahyalinodot and M. Eral, *J. Nucl. Mater.*, 2010, **396**, 251-256.
- 6 A. M. Donia, A. A. Atia, A. M. Daher, O. A. Desouky and E. A. Elshehy, *J. Radioanal. Nucl. Chem.*, 2011, **290**, 297-306.
- 7 T. S. Anirudhan and S. R. Rejeena, *Ind. Eng. Chem. Res.*, 2011, **50**, 13288-13298.